Biochemical and Biophysical Research Communications 379 (2009) 139–144

Contents lists available at ScienceDirect

Biochemical and Biophysical Research Communications

journal homepage: www.elsevier.com/locate/ybbrc

Insight into estrogenicity of phytoestrogens using *in silico* simulation

Hajime Sugiyama [a,b], Takuya Kumamoto [c], Akiko Suganami [a], Waka Nakanishi [c], Yoshihiro Sowa [d], Masaki Takiguchi [b], Tsutomu Ishikawa [c], Yutaka Tamura [a,*]

[a] Department of Bioinformatics, Graduate School of Medicine, Chiba University, Chiba 260-8670, Japan
[b] Department of Biochemistry and Genetics, Graduate School of Medicine, Chiba University, Chiba 260-8670, Japan
[c] Laboratory of Medicinal Organic Chemistry, Graduate School of Pharmaceutical Sciences, Chiba University, Chiba 263-8522, Japan
[d] Department of Molecular-Targeting Cancer Prevention, Graduate School of Medical Science, Kyoto Prefectural University of Medicine, Kyoto 602-8566, Japan

ARTICLE INFO

Article history:
Received 4 December 2008
Available online 25 December 2008

Keywords:
Estrogen receptor
Phytoestrogen
Miroestrol
in silico simulation
Docking
Molecular dynamics
Linear interaction energy

ABSTRACT

Phytoestrogens, including miroestrol and deoxymiroestrol, have the ability to act through competition with estrogen for binding to the estrogen receptor (ER). Here, we utilize manual ligand docking followed by molecular dynamics simulations and binding free energy calculations with the linear interaction energy method to predict the binding modes and the binding affinities of phytoestrogens on the ligand binding domain of ER (ERα-LBD). The calculations brought about the good correlation between the calculated binding free energy and the bioassays. Furthermore, consideration of Lennard–Jones and Coulomb interaction energies of miroestrol and deoxymiroestrol on ERα-LBD provided the information to develop the phytoestrogen derivatives as the preferred drug for ER positive breast cancer treatment.

In Thailand, *Pueraria mirifica*, an indigenous herb belongs to the Family Leguminosae, is considered to be a rejuvenating folk medicine. *P. mirifica* contains miroestrols, particularly miroestrol and deoxymiroestrol, which make difference to any other phytoestrogen-containing plants in the Family Leguminosae [1–3]. Miroestrols are an isoflavonoid compound which has the chemical structure similar to female estrogenic hormones, estradiol [4]. However, unlike 17β-estradiol, miroestrol and deoxymiroestrol are not steroidal compounds. Chansakaow et al. isolated and identified deoxymiroestrol from the root of *P. mirifica*, and concluded that it is more likely to be the actual chemical constituent of *P. mirifica* because of its facile aerial oxidization into miroestrol [5]. Other compounds found in *P. mirifica* that belong to isoflavone and coumestran groups of phytoestrogens are genistein, daidzein, daidzin, genistin and coumestrol.

Breast cancer occurs in both men and women, although male breast cancer is rare.

New cases and deaths from breast cancer in the United States in 2008 were estimated as below; new cases: 182,460 (female); 1990 (male), deaths: 40,480 (female); 450 (male) (http://www.cancer.gov/cancertopics/types/breast). Interest in phytoestrogens has been fueled by epidemiologic studies that have suggested low incidence of breast cancer in countries with high soy intake. However, this has been followed by in vitro and in vivo animal research suggesting a potential role for phytoestrogens in preventing breast cancer development, the role of phytoestrogens in breast cancer remains controversial [6]. Matsumura et al. have compared the estrogen agonist and antagonist activity of eight phytoestrogens (genistein, daidzein, equol, miroestrol, deoxymiroestrol, 8-prenylnaringenin, coumestrol and resveratrol) in a range of assays all based within the same receptor and cellular context of the MCF7 human breast cancer cell line [7].

In the present study, manual docking, molecular dynamics (MD) simulations and the linear interaction energy (LIE) method are combined to predict binding modes and estimate the binding free energies of protein–ligand interactions [8–11]. Therefore, we attempted to establish *in silico* screening methodology for the development of phytoestrogen derivatives as the preferred drug for ER positive breast cancer treatment [12]. The predicted binding affinities of phytoestrogens on the ligand binding domain of ER by *in silico* screening methodology were compared with the bioassay data of Matsumura et al. [7]. Thus consideration of an ongoing need for breast cancer drugs with greater efficacy and fewer side effects made us insight into estrogenicity of phytoestrogens [13].

Abbreviations: ER, estrogen receptor; LBD, ligand binding domain; MD, molecular dynamics; LIE, linear interaction energy; RMSD, root-mean-square deviation

* Corresponding author. Fax: +81 43 226 2544.
E-mail address: yutaka_tamura@faculty.chiba-u.jp (Y. Tamura).

0006-291X/$ - see front matter © 2008 Elsevier Inc. All rights reserved.
doi:10.1016/j.bbrc.2008.12.046

Materials and methods

Preparation and MD simulations of protein–ligand complexes. Construction of the ligand binding domain of estrogen receptor alpha (ERα-LBD) with ligand complexes and subsequent molecular dynamics (MD) simulations were performed as described before with some modifications [11]. Briefly, ERα-LBD (residues M294 to S554) was taken from the Protein Data Bank (PDB ID; 3ERD), and then several optimizations prior to MD simulations were carried out by using Modeler 8.2 [14] and Reduce 2.21 [15]. For all ligands (17β-estradiol, deoxymiroestrol, miroestrol, 8-prenylnaringenin, genistein, coumestrol, equol, daidzein, raloxifene-core, OBCP-1M and WAY-244), the force fields parameters were taken from the general Amber force field (GAFF) [16], whereas the atomic partial charges were derived by semi-empirical AM1 calculations with MOPAC2006 (Fujitsu Ltd., Japan), to which the charges were fitted using the AM1-BCC procedure [17]. Ligands were placed in the binding site of ERα-LBD by manual docking (Fig. 1) using CAChe 6.1 (Fujitsu Ltd., Japan). All MD simulations were carried out on ERα-LBD/ligand complexes using the GROMACS 3.3.1 [18] after minimization using MM2 force field in CAChe 6.1 (Fujitsu Ltd., Japan). The minimum distance between the complex and the boundaries was 6 Å, resulting in typical box volume sizes of about 9.87×10^5 Å^3, and contained ca. 100,000 atoms including ERα-LBD and ligand. Simulations of free ligands in water were carried out under periodic boundary conditions with a minimum distance between the ligand and the boundaries of 10 Å, resulting in a box volume of about 3.2×10^4 Å^3 with ca. 3300 atoms. Stepwise heating (35 ps), equilibration (750 ps) and subsequent MD simulations (250 ps) were carried out as described for ERα-LBD/ligand complexes and free-ligands. Subsequently, the stepwise heating protocol was used to relax water molecules in the systems [19].

The linear interaction energy calculations. The linear interaction energy (LIE) method was used to calculate binding free energies from the MD simulations [8–11]. Lennard–Jones (LJ) and Coulomb interaction energies between the ligand and its environment were collected to obtain the values of calculated binding free energy (ΔG_{calc}) during MD simulation. These energies were averaged every 0.2 ps from the 250 ps production run. Subsequently, Binding free energies (ΔG_i) were calculated for any orientation by

$$\Delta G_i = \alpha\left(E^{LJ}_{BOUND,i} - E^{LJ}_{FREE,i}\right) + \beta\left(E^{Coul}_{BOUND,i} - E^{Coul}_{FREE,i}\right) = \alpha\Delta E^{LJ}_i + \beta\Delta E^{Coul}_i$$

where E^{LJ} and E^{Coul} denotes the LJ interaction energy and the Coulomb interaction energy of the ligand bound to the receptor (BOUND) and the ligand free in solution (FREE), respectively. The parameters $\alpha = 0.82$ and $\beta = 0.20$ were used [11]. LJ interactions were calculated using a twin-range cutoff.

Short-range interactions (within 11 Å) were evaluated every time step from a pair list that was updated every 5 time steps. Longer-range interactions (within 12 Å) were evaluated every 5 time steps as well and kept constant between updates. A long-range correction for the finite cutoff of LJ potential was taken into account for energy and pressure corrections, but not for the binding free energy afterward. The particle mesh Ewald summation method was used for long-range electrostatic interactions [20].

Results

Confirmation of our methodology

We attempted to confirm whether manual ligand docking followed by molecular dynamics (MD) simulations and binding free energy calculations with the linear interaction energy (LIE) method reproduces same binding mode with the crystallographic structure of the ligands (17β-estradiol; 3ERD, genistein; 1X7R, raloxifene; 2JFA, OBCP-1M; 2B1V, WAY-244; 1X7E) that were complex with ligand binding domain of ER alfa (ERα-LBD) [8–11]. As shown in Fig. 2(A–E), the orientation with the best interaction energy of them closely reproduced the crystallographic structure of the pro-

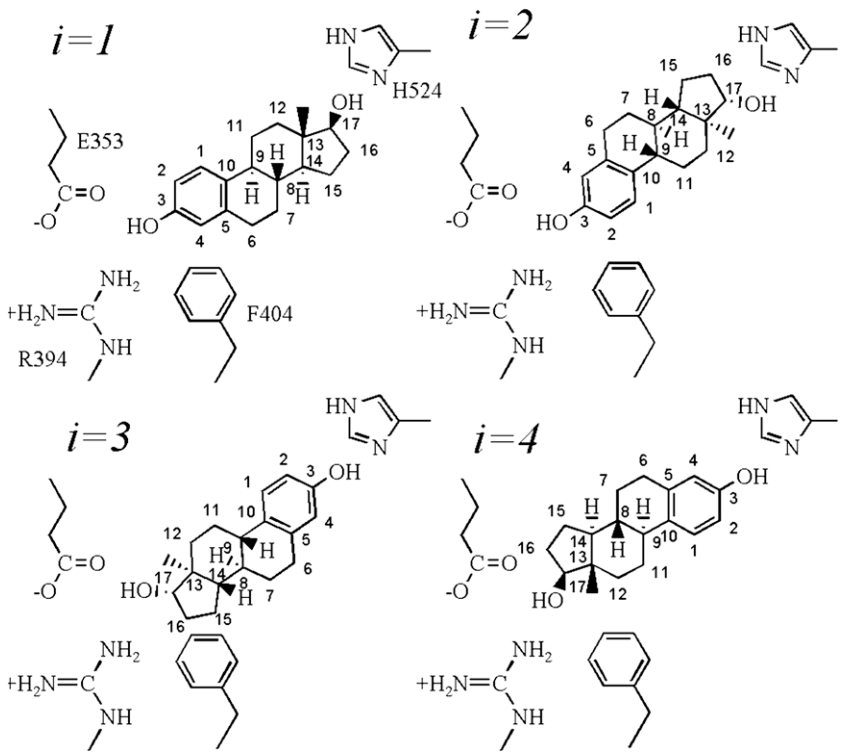

Fig. 1. Schematic view of four ligand docking orientations used in the present study. Example for 17β-estradiol.

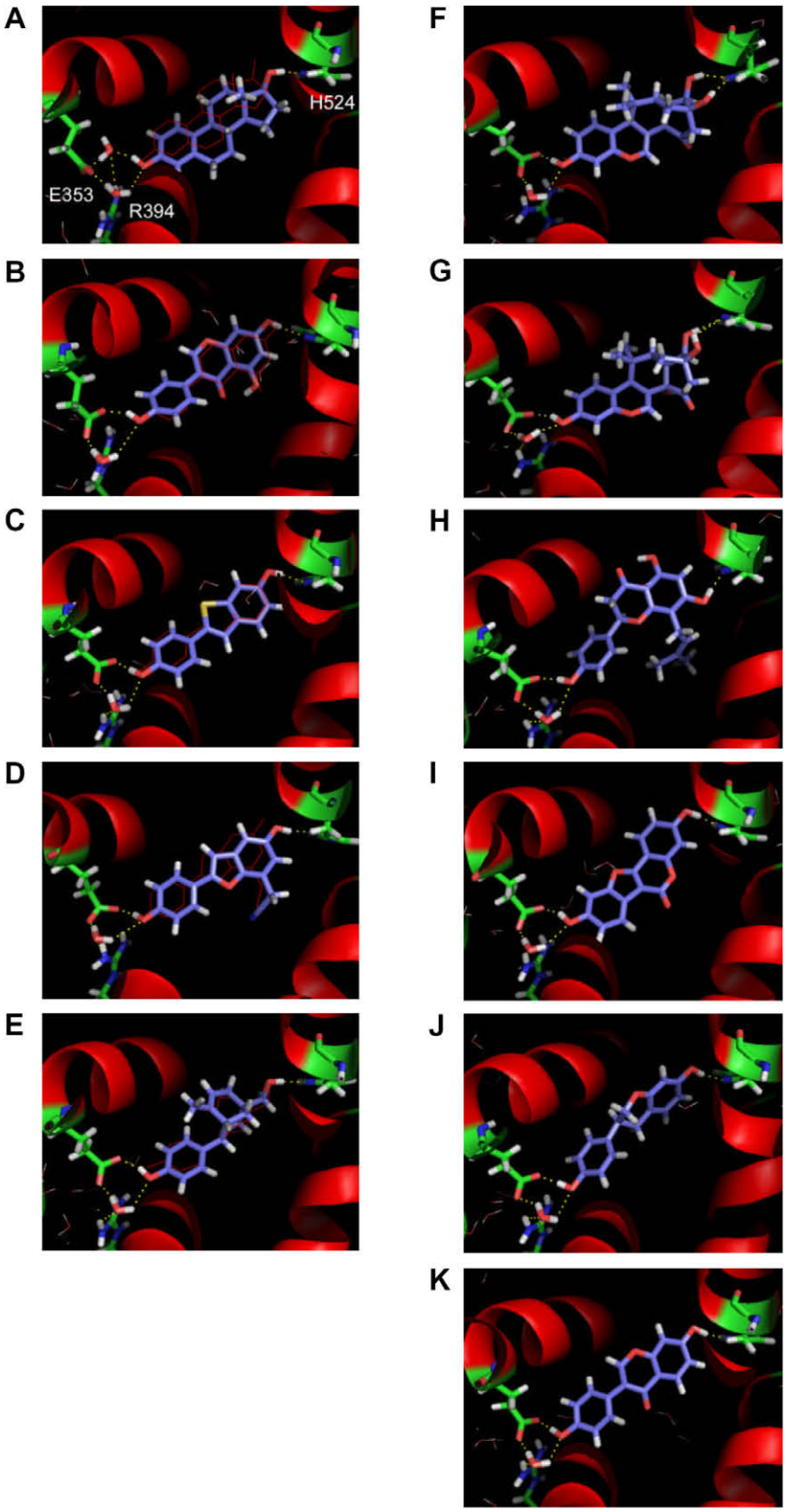

Fig. 2. Overlay of X-ray and predicted poses of ligands on ER-LBD. (A) 17β-Estradiol, (B) genistein, (C) raloxifene core, (D) OBCP-1M, and (E) WAY-244. Each predicted structures were fitted to the protein bound crystal structure merged into the reference protein coordinates. The crystal structure of the ligand (red) is compared to the average structure during MD simulations (CPK colors). Predicted pose of ligands on ER-LBD. (F) Deoxymiroestrol, (G) miroestrol, (H) 8-prenylnaringenin, (I) coumestrol, (J) equol, and (K) daidzein.

tein–ligand complex. The RMSDs of each ligand relative to that in the crystallographic structure of the protein–ligand complex were 0.26 Å for 17β-estradiol, 0.31 Å for genistein, 0.21 Å for raloxifene core, 0.40 Å for OBCP-1M and 0.25 Å for WAY-244. In the most

cases, hydrogen bonding with E353, R394, and H524 was observed for the orientation with the best interaction energy as listed in Table 1. Analysis of the RMSD values of the heavy atoms of several selected amino acid residues of the binding cavity (M343, L346, L349, A350, *E353*, L384, L387, M388, L391, *R394*, F404, L424, G521, *H524*, L525) showed even smaller variations: average RMSD = 0.98 ± 0.1 Å. This indicates that the orientation and conformation of the amino acids directly involved in ligand binding was also well-preserved.

Prediction of binding structure by our methodology

We applied the manual docking, MD simulations and LIE methods on the prediction of the binding mode and the interaction energy of structure unsolved miroestrols. Fig. 2(F–K) shows the binding mode with the best interaction energy of deoxymiroestrol, miroestrol, 8-prenylnaringenin, coumestrol, equol and daidzein complex with ERα-LBD, respectively. These predicted structures were consistent with the binding mode with structure-known ligands as shown in Fig. 2(A–E). For example, the OH groups of six miroestrols were predicted to form hydrogen bond with E353 and H524. Furthermore, all predicted binding modes of six miroestrols reproduced perpendicular π-stacking conformations of F404 and the aromatic moiety of a ligand which contributes significantly to the binding energy [21]. Finally, hydrogen bonds through a water molecule to E353 were presented.

Evaluation of predicted interaction energies by bioassays

To evaluate *in silico* screening methodology described in this study, we have plotted the predicted interaction energies of phytoestrogens complex with ERα-LBD against the experimental agonist activity of them by Matsumura et al. [7]. Fig. 3 shows the correlation of the interaction energy versus the estrogen-sensitive reporter gene assay with an $R^2 = 0.79$ (Fig. 3A) and cell growth assay with an $R^2 = 0.86$ (Fig. 3B), respectively [22].

Table 1
Overview of the Lennard–Jones (E^{LJ}) and Coulomb (E^{Coul}) interaction energy.

Ligand	Orientation in Fig. 1 (*i*=)	Bound		Free		ΔG_i	p_i
		E^{LJ}	E^{Coul}	E^{LJ}	E^{Coul}		
17β-Oestradiol	1	−32.6	−21.4	−21.1	−28.0	−11.2	0.99
	2	−34.8	−13.8			−8.4	0.01
	3	−32.2	−21.4			−7.8	0.00
	4	−33.2	−18.1			−7.9	0.00
Genistein	1	−31.3	−29.3	−18.3	−36.8	−9.1	0.69
	2	−27.2	−25.4			−5.0	0.00
	3	−29.4	−34.7			−8.6	0.30
	4	−28.2	−29.3			−6.6	0.01
Raloxifene core	1	−32.4	−24.9	−18.9	−34.4	−8.1	0.41
	2	−31.7	−20.0			−7.5	0.15
	3	−31.8	−22.5			−8.0	0.36
	4	−31.5	−23.3			−7.1	0.09
OBCP-1M	1	−32.1	−20.2	−18.5	−30.0	−9.2	0.74
	2	−31.0	−19.6			−8.2	0.13
	3	−31.9	−15.1			−7.2	0.03
	4	−30.5	−16.9			−8.0	0.10
WAY-244	1	−28.2	−22.9	−16.7	−29.7	−9.1	0.69
	2	−27.8	−21.5			−7.6	0.05
	3	−27.0	−23.2			−8.1	0.12
	4	−28.3	−22.1			−8.2	0.14
Deoxymiroestrol	1	−40.0	−29.0	−21.4	−45.3	−12.0	0.98
	2	−34.8	−32.9			−8.5	0.00
	3	−36.8	−28.0			−9.1	0.01
	4	−37.1	−24.4			−8.7	0.00
Miroestrol	1	−39.9	−29.1	−19.8	−56.7	−11.0	0.81
	2	−37.0	−28.9			−8.5	0.01
	3	−36.5	−37.6			−9.8	0.12
	4	−37.8	−29.9			−9.4	0.06
8-Prenylnaringenin	1	−40.4	−26.0	−23.9	−37.7	−11.2	0.75
	2	−39.4	−19.7			−9.2	0.02
	3	−39.7	−23.7			−10.2	0.13
	4	−41.4	−15.3			−9.9	0.09
Coumestrol	1	−28.6	−28.0	−18.4	−35.7	−6.8	0.15
	2	−30.2	−23.4			−7.2	0.28
	3	−28.5	−30.0			−7.2	0.27
	4	−29.7	−25.4			−7.2	0.29
Equol	1	−28.7	−28.8	−17.4	−32.6	−8.5	0.38
	2	−29.9	−23.4			−8.4	0.33
	3	−29.5	−24.6			−8.3	0.27
	4	−26.8	−27.1			−6.6	0.02
Daidzein	1	−25.9	−25.8	−16.8	−39.4	−4.7	0.00
	2	−28.6	−30.5			−7.9	0.60
	3	−27.4	−33.8			−7.6	0.35
	4	−28.2	−24.4			−6.4	0.05

All ΔE and ΔG values are given in kcal/mol.

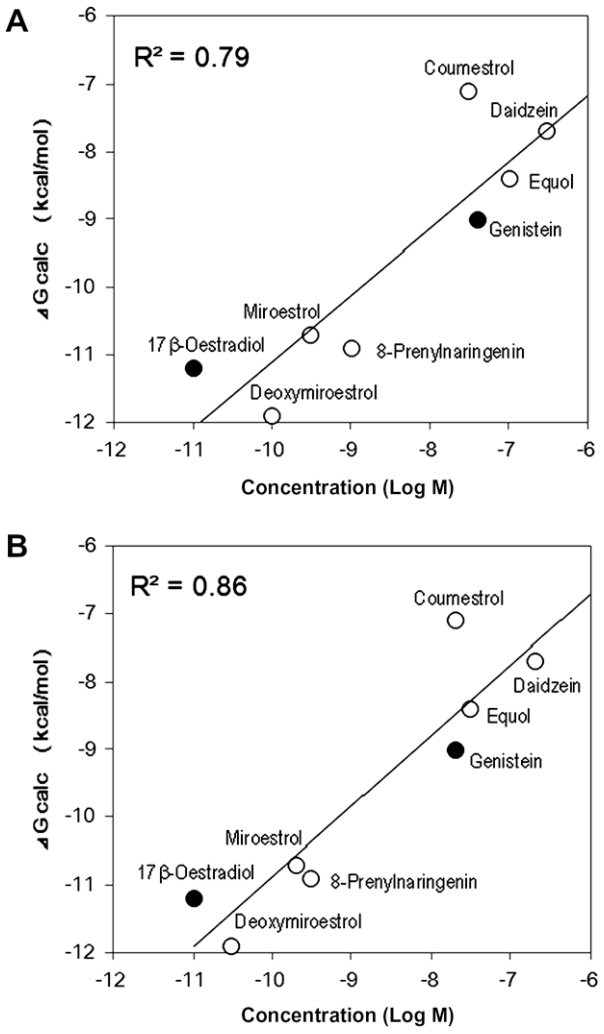

Fig. 3. Comparison of the predicted free energy of binding versus experimental agonist activity for the eight ligands. The *X*-axis value of panel A and B were derived from ERE-CAT and cell proliferation assay, respectively.

Difference of binding affinity between deoxymiroestrol and miroestrol

To understand why deoxymiroestrol provides a significant increase in affinity and antagonist potency compared to miroestrol, we performed the detail consideration of Lennard–Jones (LJ) and Coulomb interaction energies between the ligand and its environment. As summarized in Table 2A, the sum of contribution in bound state for deoxymiroestrol of −38.5 kcal/mol is slightly stronger than that for miroestrol of −38.3 kcal/mol. On the other hand, the sum of penalty in free state for deoxymiroestrol of −26.6 kcal/mol is weaker than that for miroestrol of −27.6 kcal/mol (Table 2B). Therefore, these results mean that the affinity of deoxymiroestrol on ERα-LBD is 1.2 kcal/mol stronger than that of miroestrol.

Table 2A
Energy contributions in bound states for calculated binding free energy of deoxymiroestrol, miroestrol, and the difference. All units are kcal/mol.

	Deoxymiroestrol	Miroestrol
$\alpha\Delta\bar{E}^{LJ}_{BOUND}$	−32.7	−32.3
$\beta\Delta\bar{E}^{Coul}_{BOUND}$	−5.8	−6.0
$\alpha\Delta\bar{E}^{LJ}_{BOUND} + \beta\Delta\bar{E}^{Coul}_{BOUND}$	−38.5	−38.3

Table 2B
Energy contributions in free states for calculated binding free energy of deoxymiroestrol, miroestrol, and the difference. All units are kcal/mol.

	Deoxymiroestrol	Miroestrol
$\alpha\Delta\bar{E}^{LJ}_{FREE}$	−17.5	−16.3
$\beta\Delta\bar{E}^{Coul}_{FREE}$	−9.1	−11.3
$\alpha\Delta\bar{E}^{LJ}_{FREE} + \beta\Delta\bar{E}^{Coul}_{FREE}$	−26.6	−27.6

Discussion

The aim of this study is to establish *in silico* screening methodology for the development of phytoestrogen derivatives as the preferred drug for ER positive breast cancer treatment [19,23–25]. We have performed *in silico* screening consists of manual ligand docking followed by MD simulations and binding free energy calculations with LIE method for phytoestrogens on ERα-LBD [8–11]. The predicted binding affinities of phytoestrogens on ERα-LBD by our *in silico* screening methodology showed excellent correlation with the experiment data using a range of assays all based within the same receptor and cellular context of the MCF7 human breast cancer cell line by Matsumura et al. [7]. However, the profile of interaction energy of miroestrol and deoxymiroestrol were in pretty well agreement, the remarkable difference between them are only arising from the functional group at 14 positions. Therefore, we focused on why the functional group at 14 position of deoxymiroestrol, the highest activity of all estrogens of plant origin, plays a critical role for the binding with ERα-LBD. As the results of the calculation, the difference of contribution in bound state shows the interactions of deoxymiroestrol to ERα-LBD is stronger (0.2 kcal/mol) than that of miroestrol. On the other hand, the difference of penalty in free state showed that deoxymiroestrol has lower affinity to water (1.0 kcal/mol) as compared with miroestrol. These results indicate the interaction between the functional group at 14 position of miroestrols, miroestrol and deoxymiroestrol, and water determined the binding stability of protein–ligand complex (Fig. 4).

Finally, the facile aerial oxidation of deoxymiroestrol into miroestrol loses its highest estrogenicity in all estrogens of plant origin. Therefore, *in silico* screening methodology for the development of phytoestrogen derivatives may be a powerful tool to develop the deoxymiroestrol derivatives as the preferred drug for ER positive breast cancer treatment.

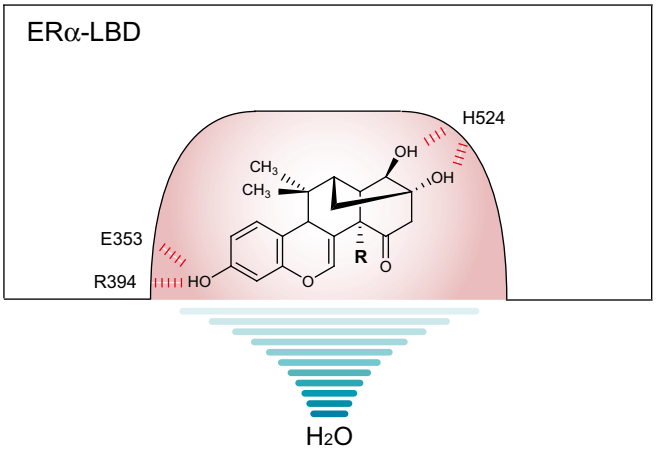

Fig. 4. Schematic presentation of the interaction of miroestrols on ERα-LBD (red) and solvent (blue). R = OH; deoxymiroestrol, R = H; miroestrol.

Acknowledgment

This work was supported by a grant from Futaba Electronics Memorial Foundation (to Y. Tamura).

References

[1] J.C. Cain, Miroestrol: an oestrogen from the plant *Pueraria mirifica*, Nature 188 (1960) 774–777.
[2] H.E. Jones, G.S. Pope, A study of the action of miroestrol and other oestrogens on the reproductive tract of the immature female mouse, J. Endocrinol. 20 (1960) 229–235.
[3] H.E. Jones, G.S. Pope, A method for the isolation of miroestrol from *Pueraria mirifica*, J. Endocrinol. 22 (1961) 303–312.
[4] L. Terenius, Structural characteristics of oestrogen binding in the mouse uterus: inhibition of 17beta-oestradiol binding in vitro by a plant oestrogen, miroestrol, Acta Pharmacol. Toxicol. (Copenh) 26 (1968) 15–21.
[5] S. Chansakaow, T. Ishikawa, H. Seki, K. Sekine, M. Okada, C. Chaichantipyuth, Identification of deoxymiroestrol as the actual rejuvenating principle of "Kwao Keur", *Pueraria mirifica*. The known miroestrol may be an artifact, J. Nat. Prod. 63 (2000) 173–175.
[6] C. Duffy, K. Perez, A. Partridge, Implications of phytoestrogen intake for breast cancer, CA Cancer J. Clin. 57 (2007) 260–277.
[7] A. Matsumura, A. Ghosh, G.S. Pope, P.D. Darbre, Comparative study of oestrogenic properties of eight phytoestrogens in MCF7 human breast cancer cells, J. Steroid Biochem. Mol. Biol. 94 (2005) 431–443.
[8] J. Carlsson, L. Boukharta, J. Aqvist, Combining docking, molecular dynamics and the linear interaction energy method to predict binding modes and affinities for non-nucleoside inhibitors to HIV-1 reverse transcriptase, J. Med. Chem. 51 (2008) 2648–2656.
[9] T. Hansson, J. Marelius, J. Aqvist, Ligand binding affinity prediction by linear interaction energy methods, J. Comput. Aided Mol. Des. 12 (1998) 27–35.
[10] M. Nervall, P. Hanspers, J. Carlsson, L. Boukharta, J. Aqvist, Predicting binding modes from free energy calculations, J. Med. Chem. 51 (2008) 2657–2667.
[11] M.M. van Lipzig, A.M. ter Laak, A. Jongejan, N.P. Vermeulen, M. Wamelink, D. Geerke, J.H. Meerman, Prediction of ligand binding affinity and orientation of xenoestrogens to the estrogen receptor by molecular dynamics simulations and the linear interaction energy method, J. Med. Chem. 47 (2004) 1018–1030.
[12] B. Fischer, K. Fukuzawa, W. Wenzel, Receptor-specific scoring functions derived from quantum chemical models improve affinity estimates for in-silico drug discovery, Proteins 70 (2008) 1264–1273.
[13] P.J. Magee, I.R. Rowland, Phyto-oestrogens, their mechanism of action: current evidence for a role in breast and prostate cancer, Br. J. Nutr. 91 (2004) 513–531.
[14] A. Fiser, A. Sali, Modeller: generation and refinement of homology-based protein structure models, Methods Enzymol. 374 (2003) 461–491.
[15] J.M. Word, S.C. Lovell, J.S. Richardson, D.C. Richardson, Asparagine and glutamine: using hydrogen atom contacts in the choice of side-chain amide orientation, J. Mol. Biol. 285 (1999) 1735–1747.
[16] J. Wang, R.M. Wolf, J.W. Caldwell, P.A. Kollman, D.A. Case, Development and testing of a general amber force field, J. Comput. Chem. 25 (2004) 1157–1174.
[17] A. Jakalian, D.B. Jack, C.I. Bayly, Fast, efficient generation of high-quality atomic charges. AM1-BCC model. II. Parameterization and validation, J. Comput. Chem. 23 (2002) 1623–1641.
[18] D. Van Der Spoel, E. Lindahl, B. Hess, G. Groenhof, A.E. Mark, H.J. Berendsen, GROMACS: fast, flexible, and free, J. Comput. Chem. 26 (2005) 1701–1718.
[19] B.C. Oostenbrink, J.W. Pitera, M.M. van Lipzig, J.H. Meerman, W.F. van Gunsteren, Simulations of the estrogen receptor ligand-binding domain: affinity of natural ligands and xenoestrogens, J. Med. Chem. 43 (2000) 4594–4605.
[20] T. Darden, D. York, L. Pedersen, Particle mesh Ewald: an *N*-log(*N*) method for Ewald sums in large systems, J. Chem. Phys. 98 (1993) 10089–10092.
[21] S. Tsuzuki, K. Honda, R. Azumi, Model chemistry calculations of thiophene dimer interactions: origin of pi-stacking, J. Am. Chem. Soc. 124 (2002) 12200–12209.
[22] J.R. Byford, L.E. Shaw, M.G. Drew, G.S. Pope, M.J. Sauer, P.D. Darbre, Oestrogenic activity of parabens in MCF7 human breast cancer cells, J. Steroid Biochem. Mol. Biol. 80 (2002) 49–60.
[23] S. Bjelic, M. Nervall, H. Gutierrez-de-Teran, K. Ersmark, A. Hallberg, J. Aqvist, Computational inhibitor design against malaria plasmepsins, Cell. Mol. Life Sci. 64 (2007) 2285–2305.
[24] H. Gutierrez-de-Teran, M. Nervall, B.M. Dunn, J.C. Clemente, J. Aqvist, Computational analysis of plasmepsin IV bound to an allophenylnorstatine inhibitor, FEBS Lett. 580 (2006) 5910–5916.
[25] T. Jain, B. Jayaram, An all atom energy based computational protocol for predicting binding affinities of protein–ligand complexes, FEBS Lett. 579 (2005) 6659–6666.